Quaternary Research (2024), 1–16
doi:10.1017/qua.2024.23

Research Article

Understanding the fluvial capture of the Guadix-Baza Basin in SE Spain through its oldest exorheic deposits

Francisco J. García-Tortosa[a], Pedro Alfaro[b], Iván Martin-Rojas[b], Iván Medina-Cascales[b] and Santiago Giralt[c]

[a]Departamento de Geología, Universidad de Jaén, Campus Las Lagunillas s/n, 23071 Jaén, Spain; [b]Departamento de Ciencias de la Tierra y del Medio Ambiente, Universidad de Alicante, 03690 San Vicente del Raspeig, Alicante, Spain and [c]Geosciences Barcelona (GEO3BCN), CSIC, Lluís Solé i Sabarís s/n, 08028 Barcelona, Spain

Abstract

The fluvial capture of endorheic basins represents a milestone in basin chronology, implying a profound disequilibrium that triggers critical geomorphological, sedimentological, paleogeographic, and even paleoecological transformations. The primary goal of many geomorphological studies is to determine the timing of endorheic-to-exorheic transitions with the objective of unveiling the dynamics that follow the capture event. The age of the Guadix-Baza Basin capture in the Central Betic Cordillera (S Spain) remains a subject of controversy, with proposed estimates ranging from 17 to 600 ka. In this study, we present new $^{234}U/^{230}Th$ and optically stimulated luminescence ages from exorheic deposits exposed within the basin's main fluvial valley, the Guadiana Menor River. We acquired the oldest numerical age recorded to date for a postcapture deposit within the basin. This age corresponds to a travertine platform formed 240.8 ± 25 ka on a surface level that was already incised into the glacis surface at approximately 250 m. Using these data, we estimate that basin capture took place earlier than ca. 240 ka, plus the time required for the river to incise 250 m to the position of the travertine. Furthermore, the proximity of the Matuyama-Brunhes reversal (781 ka) to the top of the endorheic succession and the ages of the paleontological sites (> ca. 750 ka) throughout the basin suggest that the capture could have occurred earlier than the oldest previously proposed age of 600 ka.

Keywords: Fluvial capture, Landscape evolution, Iberia, Granada Geopark

(Received 22 September 2023; accepted 22 April 2024)

Introduction

Endorheic basins, also known as closed or internally drained basins, are subject to intensive research, because they provide important insights into the evolution of sedimentary basins, climate changes, or tectonic processes (Mather, 2000; García Castellanos et al., 2003; Sobel et al., 2003; García Castellanos and Cruz Larrasoaña, 2015; Heidarzadeh et al., 2017; Bridgland et al., 2020; among many others). There are only a few examples of outcropping Quaternary continental records of endorheic basins (e.g., Silva et al., 2017; Stokes et al., 2018; Bridgland et al., 2020). This lack of outcropping endorheic basins occurs because, apart from drilling and geophysical surveys, such information is revealed only once the sedimentary record of the basin has been exposed, which implies the dissection of the basins by river networks during a subsequent exorheic phase. Therefore, the capture of an endorheic basin is a major milestone in its landscape evolution (e.g., Merritts et al., 1994; García Castellanos et al., 2003; Arboleya et al., 2008; Struth et al., 2019). Consequently, the detailed characterization of these basins is crucial to fully understand the contribution and interplay of tectonic and climate processes in their sedimentary filling, as well as the erosion dynamics during their later exorheic stages.

The Guadix-Baza Basin (GBB) is an example of a Plio-Quaternary endorheic basin that was captured and subsequently dissected by river incision and slope erosion during the Quaternary period (Fig. 1). Extensive sedimentation during the endorheic stage produced a continuous continental sedimentary succession that was several hundred meters thick. This succession represents the most well-preserved and accessible continental Plio-Quaternary stratigraphic record in Europe. This record includes more than 150 paleontological sites of vertebrates (Agustí, 1986; Alberdi and Bonadonna, 1989; Agustí et al., 2015; Maldonado-Garrido et al., 2017; among many others). Moreover, the paleontological record of the GBB also comprises the oldest human fossils of western Europe (Toro-Moyano et al., 2013) and some of the oldest stone tool industries in Europe (also older than 1 Ma; Toro-Moyano et al., 2011). After the transition from endorheic to exorheic conditions (Calvache and Viseras, 1997), extensive deposition in the basin ended and was replaced by intense incisions of the fluvial network into the flat top surface of the basin (glacis surface; sensu García-Tortosa et al., 2008b). The new base level (Atlantic

Corresponding author: Francisco J. García-Tortosa; Email: gtortosa@ujaen.es

Cite this article: García-Tortosa FJ, Alfaro P, Martin-Rojas I, Medina-Cascales I, Giralt S (2024). Understanding the fluvial capture of the Guadix-Baza Basin in SE Spain through its oldest exorheic deposits. *Quaternary Research* 1–16. https://doi.org/10.1017/qua.2024.23

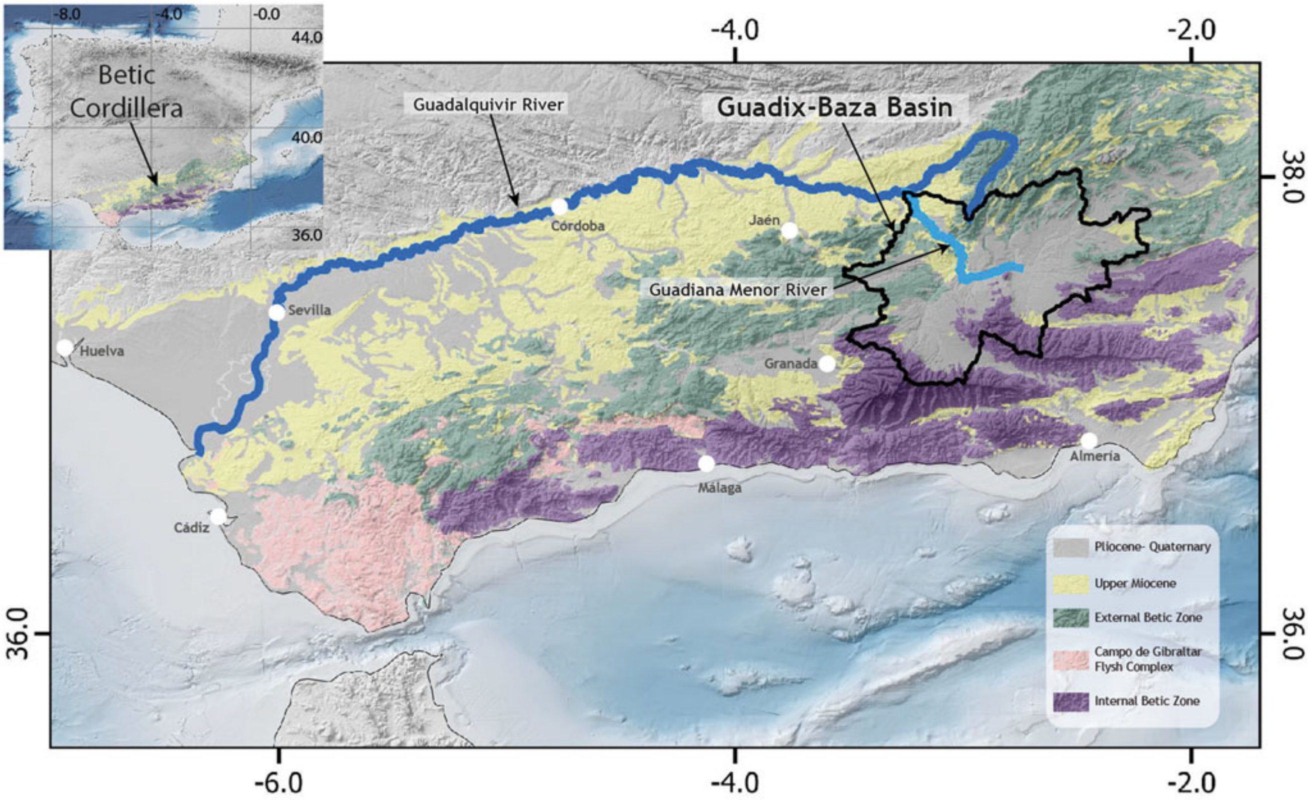

Figure 1. Geologic map of the Betic Cordillera showing the location of the Guadix-Baza Basin (GBB). The Guadiana Menor River (the main river of the GBB) and the Guadalquivir River are also depicted.

Ocean) triggered an intense fluvial network incision in the basin that reached a maximum of 300 m below the glacis surface (Fig. 2). However, although the capture of the GBB is a major event that configured most of the critical features of the basin, the age of this process remains elusive.

In this work, we provide the oldest numerical ages obtained thus far for exorheic deposits in the GBB. We integrate these results with previously reported data for the youngest endorheic deposits to discuss the age of the capture. Our results not only provide crucial information for the geologic history of the GBB but also permit a more general approach that can be applied to other internally drained basins and that will help in understanding how these basins were captured and subsequently reshaped. Furthermore, our conclusions enhance the understanding of both geologic and geomorphic settings of some of the most relevant archaeological and paleontological sites in Europe.

Geologic Setting

The GBB is an intramontane basin more than 4000 km^2 in size located in the Central Betic Cordillera (SE Spain; Figs. 1 and 3). This region undergoes active tectonic deformation related to the 5 mm/yr, NNW–SSE convergence between the Nubian and Eurasian plates (DeMets et al., 1994; Serpelloni et al., 2007; Nocquet, 2012). As a result, the Central Betic Cordillera experiences NNW–SSE shortening (Sanz de Galdeano, 1983) and ENE–WSW orthogonal extension (Galindo-Zaldívar et al., 2015; Martin Rojas et al., 2023). This deformation is responsible for the formation of several active faults and folds and for the high mean altitude of the GBB (ca. 1000 m above sea level).

Active structures deform the Pliocene and Quaternary infill of the GBB (Alfaro et al., 2008, 2021; García-Tortosa et al., 2008b, 2011; Fernández-Ibáñez et al., 2010; Sanz de Galdeano et al., 2012; Castro et al., 2018; Medina-Cascales et al., 2020; Fig. 3), leading to a heterogeneous basin architecture characterized by tectonically uplifted and lowered areas (García-Tortosa et al., 2011). The most significant active structure is the east-dipping, normal Baza Fault (Fig. 3), whose total cumulative displacement has exceeded 2000 m since the late Miocene (Alfaro et al., 2008). The slip rates reported for this active fault range between 0.3 ± 0.3 and 1.3 ± 0.4 mm/yr (Alfaro et al., 2008, 2021; García-Tortosa et al., 2008b, 2011). The regional ENE-WSW extension accommodated by these faults has characterized the geodynamic setting of the GBB during the Pliocene and Quaternary (Martin Rojas et al., 2023). In the case of the Baza Fault, no significant change in the slip rate has been described during the Quaternary.

The displacement of the Baza Fault is responsible for some of the major geologic and geomorphic features of the GBB (García-Tortosa et al., 2008b, 2011), the most remarkable being the division of the GBB into two sectors: the eastern sector (Baza Subbasin), located on the fault downthrown block, and the western sector (Guadix Subbasin), located on the fault upthrown block.

The endorheic–exorheic transition of the GBB

The Plio-Quaternary geologic, sedimentological, and geomorphological evolution of the GBB is divided into two main stages (Fig. 4): a first endorheic stage and a subsequent exorheic stage.

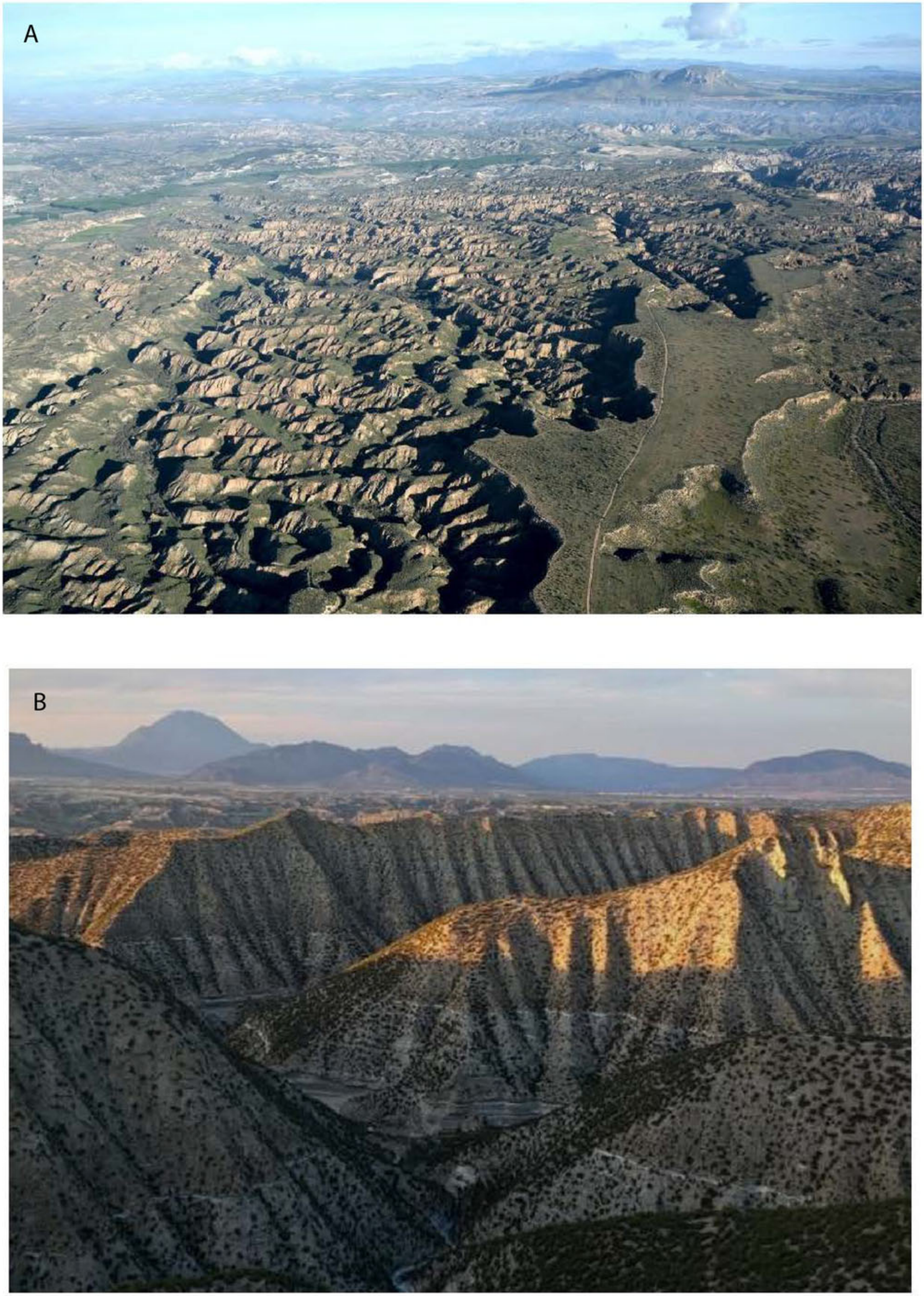

Figure 2. Oblique panoramic views of the badlands landscape of the Guadix-Baza Basin (GBB). The flat elevated surface is the glacis. (**a**) Western sector; (**b**) eastern sector.

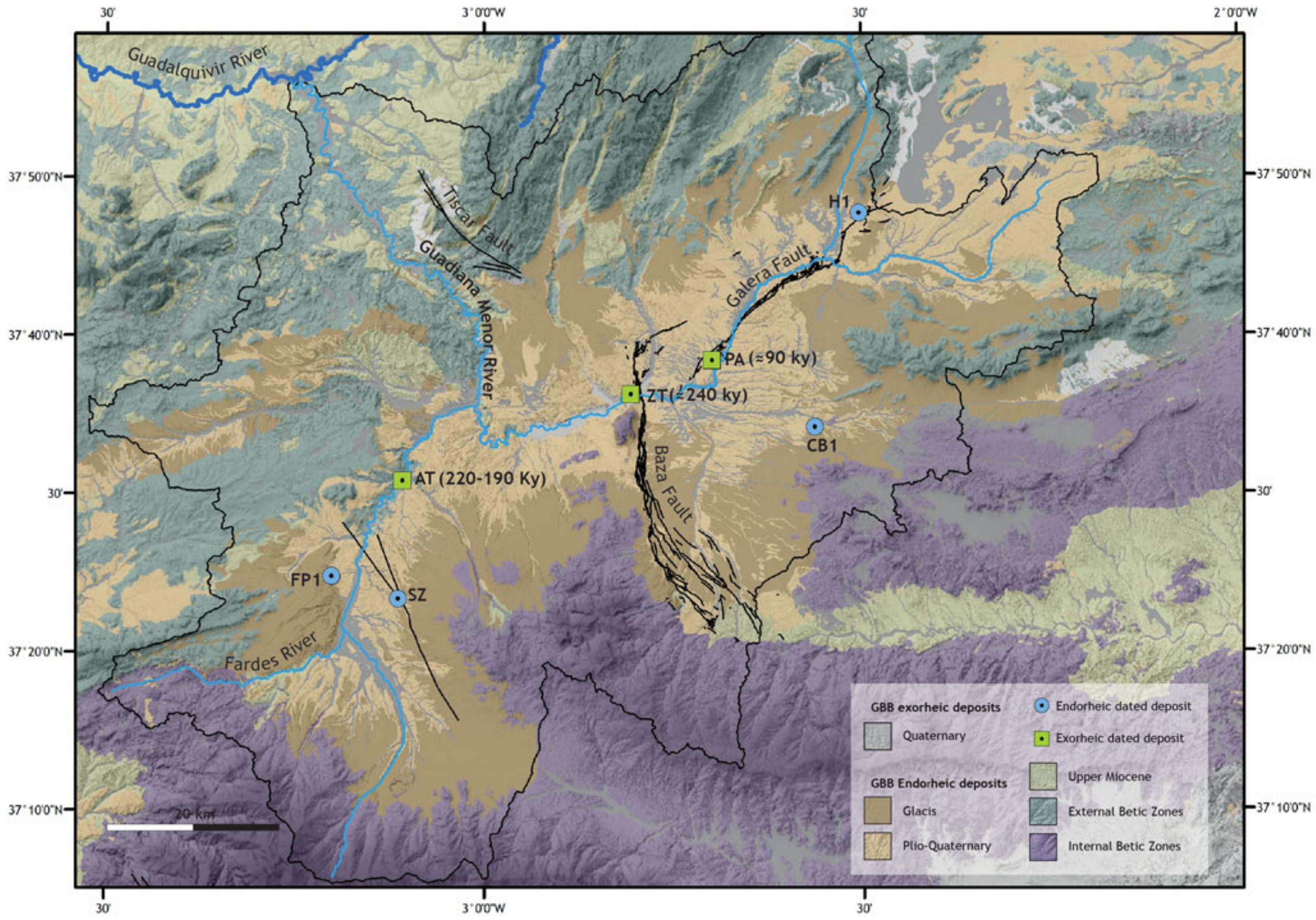

Figure 3. Geologic map of the Guadix-Baza Basin (GBB) showing the locations of the dated deposits and paleontological sites mentioned in this study. FP1, Fonelas P-1 paleontological site; CB1, Cúllar-Baza 1 paleontological site; H1, Huéscar 1 paleontological site; SZ, Solana del Zamborino paleontological site; AT, Alicún travertines; ZT, Zújar travertines; PA, Puente Arriba fluvial terrace. The black traces represent active faults, including the Baza Fault.

The transition between the endorheic and exorheic stages took place when the GBB was captured by an outer fluvial system.

The endorheic stage and subsequent continental sedimentation in the GBB began at the end of the late Miocene, when the basin was disconnected from the Atlantic Ocean and the Mediterranean Sea (Soria et al., 1999). During this endorheic stage, the Baza Fault conditioned the sedimentary environments of the basin. In the downthrown eastern sector, a lake (Baza paleo-Lake) developed (Alfaro et al., 2008; García-Tortosa et al., 2008b). This lake was gradually filled by a thick lacustrine sedimentary succession (Vera, 1970; Peña, 1985; Gibert et al., 2007a). Moreover, the upthrown western sector was dominated by fluvial systems and, thus, detrital sedimentation (Vera, 1970; Viseras, 1991). The main river of the western fluvial system was the Fardes paleo-River (Calvache and Viseras, 1997; Fig. 4). This river drained from W to E toward paleo-Lake Baza, the main depocenter of the basin (Fig. 4). The Fardes paleo-River outlet into the Baza paleo-Lake was located to the north of Jabalcon Mountain (Fig. 4), where an alternation of fluvial and lacustrine sediments is observed. This interdigitation is located in the transition zone between the western fluvial sector and the eastern lacustrine sector.

A top basin glacis developed in the GBB at the end of its endorheic stage (García-Tortosa et al., 2008b, 2011), extending almost the entire basin (Figs. 3 and 4). This glacis presents a mixed depositional/erosive nature (García-Tortosa et al., 2008b), with erosion dominating in the outer parts close to the surrounding mountains and deposition prevailing in the inner sectors of the basin. Due to this "mixed" characteristic, the endorheic deposits just below the glacis present different ages along the GBB. This geomorphological surface has been used as a marker to estimate tectonic deformation rates (García Tortosa et al., 2008b, 2011; Fernández Ibáñez et al., 2010; Sanz de Galdeano et al., 2012) and fluvial incision rates in the GBB (Pérez-Peña et al., 2009).

The glacis surface represents the youngest remaining feature of the endorheic stage. At some point during the middle Pleistocene), the exorheic stage began when the GBB was captured by the Guadiana Menor River (GMR), a tributary of the Guadalquivir River (Fig. 4) (Calvache and Viseras, 1997). Previous works focused on this capture process propose, for instance, that the area from which the basin was captured was controlled by tectonics (Calvache and Viseras, 1997; García-Tortosa et al., 2008b; Moral and Balanyá, 2020). However, no further details about the development of the capture process have been provided.

Once the basin was captured, its internal drainage was opened toward the Atlantic Ocean. The capture implied a major drop (more than 500 m) in the base level of the GBB drainage system, triggering intense headward erosion and fluvial incision processes that have dominated the basin since that moment (García-Tortosa et al., 2008a, 2008b). During the exorheic stage, sedimentation was restricted to small alluvial systems around the basin borders

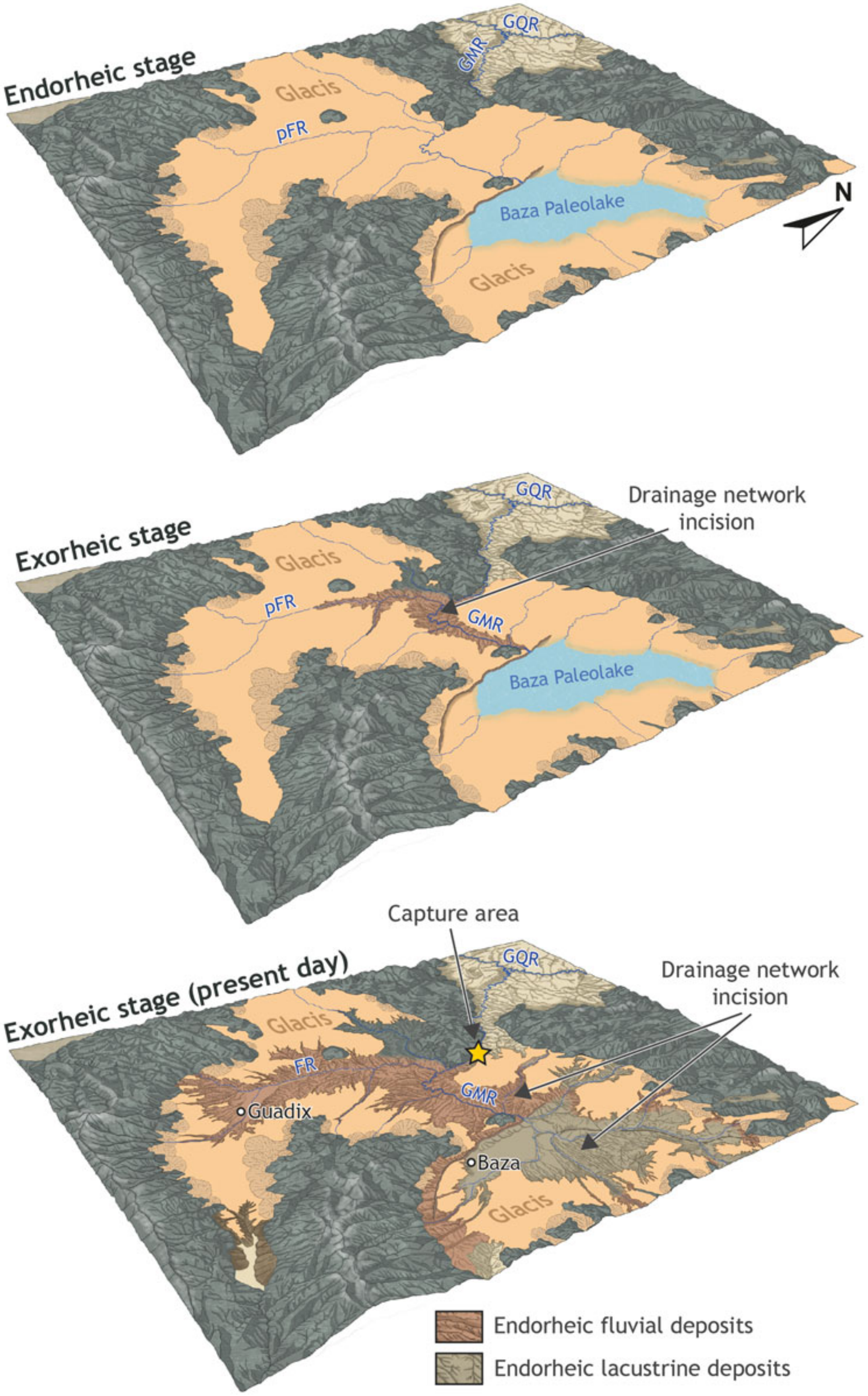

Figure 4. Sketches illustrating the Plio-Quaternary evolution of the Guadix-Baza Basin (GBB). During the initial endorheic stage, glacis developed throughout the entire basin. After the capture of the basin, the GBB became exorheic, and erosion has prevailed since that moment. pFR, Fardes paleo-River; FR, Fardes River; GQR, Guadalquivir River: GMR, Guadiana Menor River.

and to valley bottoms, resulting in the formation of several fluvial terraces at different elevations. In addition, various travertine systems, such as the Alicún travertines (Díaz-Hernández and Juliá, 2006) and the Zújar travertines, precipitated and covered some of these exorheic fluvial terraces.

The controversial age of the capture

The age of the GBB's capture must be constrained between the youngest endorheic deposit and the older exorheic deposit. To date, several works have focused on one or another of the abovementioned constraints (Peña, 1985; Calvache and Viseras, 1997; Ortiz et al., 2000; Díaz-Hernández and Juliá, 2006; Gibert et al., 2007b; García-Tortosa et al., 2008a, 2008b; Scott and Gibert, 2009). These different approaches led to controversial results, as the proposed ages for the capture range between 17 ka (Calvache and Viseras, 1997) and 600 ka (Gibert et al., 2007b; Scott and Gibert, 2009). Therefore, the age of the GBB's capture remains an open scientific debate. In this section, we describe the works focused on this debate.

Most of the research regarding the timing of capture primarily relies on lower constraints. In this way, the first group of studies focused on dating the most recent endorheic deposits or the age of the glacis surface. These ages are determined by studying several paleontological sites located at the uppermost part of the endorheic sedimentary succession, very close to the glacis.

The most used paleontological site in relation to capture has been the Solana del Zamborino site (Botella, 1975; Botella et al., 1976; Casas et al., 1976; Fig. 3). Pioneer works dated this site as ca. 100 ka (Botella, 1975; Botella et al., 1976) because of the presence of the Acheulian stone tool industry. This age was widely used as a lower constraint for the GBB's capture (Peña, 1985; Vera et al., 1994). For instance, Calvache and Viseras (1997) proposed that capture occurred between 100 and 17 ka, which corresponds to the age of several exorheic deposits (Jiménez de Cisneros, 1994). More recently, Scott and Gibert (2009) postulated an age of 750–770 ka for the Solana del Zamborino site based on the position of the Matuyama-Brunhes paleomagnetic reversal (ca. 781 ka), found just below this site, and sedimentation rates. In addition, Scott and Gibert (2009), using their sedimentation rates, proposed an approximate age of 600 ka for the glacis surface and thus for the basin's capture. Using a similar approach but different sedimentation rates, Álvarez Posada et al. (2017) proposed an age of 480–300 ka for the Solana del Zamborino site.

Another paleontological site used to constrain the age of the capture was Cúllar-Baza 1 (CB1), which is in the eastern sector of the GGB (Fig. 3). This site was initially dated as younger than ca. 750 ka (Ruiz Bustos, 1976; Alberdi and Bonadonna, 1989; Agustí et al., 1999; Gibert et al., 2007b; among others). This age agrees with later magnetostratigraphic analyses that placed the Matuyama-Brunhes reversal (ca. 781 ka) below the CB1 site (Gibert et al., 2007b). Furthermore, Gibert et al. (2007b) propose an age of ca. 600 ka for the glacis in the CB1 sector using the location of the Matuyama-Brunhes reversal ca. 19 m below this surface.

Further research regarding the age of the endorheic deposits was carried out by Azañón et al. (2006). These authors propose an estimated age of 43 ka for the capture event, based on $^{234}U/^{230}Th$ dating of a calcrete paleosoil located at the top surface of the basin in the western sector of the GBB, assuming that this calcrete was formed during the endorheic stage of the basin.

A second group of studies relied on dating the oldest exorheic deposits to establish a minimum age of the capture. Ortiz et al. (2000) dated an exorheic fluvial terrace with amino acid racemization. These authors postulated that GBB capture occurred earlier than 239 ka. Díaz-Hernández and Juliá (2006) did not directly propose an age for fluvial capture but estimated a time span for the development of the glacis and the river incision. For this purpose, they conducted $^{234}U/^{230}Th$ dating on several travertine platforms and calcretes in the Alicún travertines, found in the western sector of the GBB (Fig. 3, AT). In the case of these exorheic travertines, they obtained an age of ca. 220–190 ka for a platform located in a valley 190 ± 10 m below the glacis surface. For the calcrete, formed at the glacis level, the oldest sample provided an age of ca. 350 ka. From these data, they propose a timing between 350 and 205 ka for glacis development and between 115 and 48 ka for valley incision and the formation of erosive landforms.

The age of the capture has also been quantified using indirect criteria (García-Tortosa et al., 2008a, 2008b). Using the fault slip rate of the Baza Fault and the glacis offset induced by this structure, García-Tortosa et al. (2008b) postulate a minimum age of 400 ka for the GBB capture.

New Ages of Exhoreic Deposits of The GBB

Dating methods

We numerically dated exorheic deposits located along the course of the Guadiana Menor, the main river in the GBB, to better constrain the age of the capture. The studied exorheic deposits were the Zújar travertines and the Puente Arriba fluvial terrace (Figs. 3 and 5–8).

We dated the Zújar travertines using the uranium-series disintegration ($^{234}U/^{230}Th$) method (Fig. 5, Table 1). For this purpose, three samples of the travertine platforms were collected and radiometrically dated at the Geochronology Laboratory of Geosciences Barcelona (GEO3BCN–CSIC) (Table 1). The radiometric ages were obtained through alpha-spectrometry using an ORTEC OCTETE PLUS spectrometer equipped with eight BR-024-450-100 detectors. The chemical separation of the radioisotopes and purification from travertine samples (~20 g) were conducted following the procedure described by Bischoff et al. (1988), and isotope electrodeposition was performed according to the method of Talvitie (1972), modified by Hallstadius (1984). Absolute ages were obtained employing the software designed by Rosenbauer (1991).

In the Puente Arriba Terrace (PAT), we collected one sample 1.5 m below the top of this terrace for optically stimulated luminescence (OSL) dating (Fig. 7, Table 1). This sample was dated at the Laboratory of Radioisotopes at the University of Seville. Dose rates were based on the average radionuclide activities of bulk material from each sample. High-resolution gamma spectrometry was used to measure the concentrations of ^{238}U, ^{232}Th, and ^{40}K. Appropriate conversion factors (Adamiec and Aitken, 1998) were then used to derive the dose rates. A water content of 5 ± 2% was considered representative of the burial time. This value was used to calculate the attenuation of the dose. The contribution of cosmic radiation to the total dose rate was calculated as a function of latitude, altitude, burial depth, and average overburden density based on data by Prescott and Hutton (1994). Equivalent dose (D_e) values were derived from the OSL measurements of quartz grain sizes ranging from 180 to 250 μm extracted from the sample. We measured 24 to 48 multigrain aliquots (~30 grains/aliquot) by applying the SAR blue OSL protocol (Murray and Wintle, 2000).

Numerical ages of the Zújar travertines

The Zújar travertines (Figs. 5 and 6) are in the western sector of the GBB, very close to the border with the eastern sector (Fig. 3). These travertines are located ca. 35 km upstream from the area where the GMR captured the former fluvial network of the basin. This group of travertine platforms was deposited on the left bank of the GMR and appear to be related to a hydrothermal

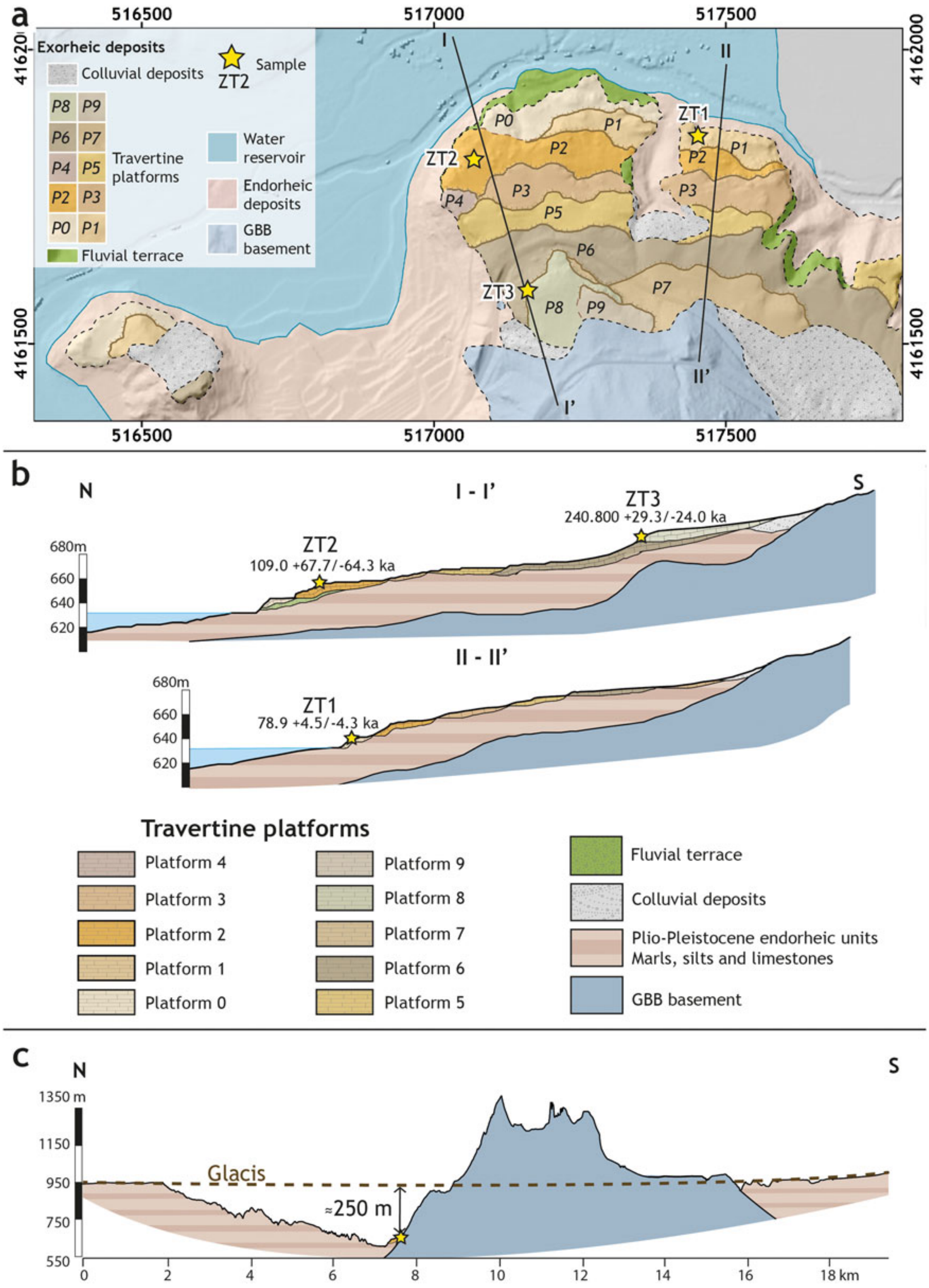

Figure 5. (**a**) Geologic map of the Zújar travertine platforms. (**b**) Geologic cross sections along the Zújar travertines (location in **a**). (**c**) Topographic profile showing the position of the Zújar travertines related to the glacis and the present thalweg. GBB, Guadix-Baza Basin.

spring, currently located 1 km to the west. This spring is characterized by a water output temperature up to 38°C and a discharge rate of 180 L/s (Cruz-Sanjulián and García-Rosell, 1972). At this position, the river valley is steeply incised into endorheic deposits. The travertine structure is made up of 10 carbonate platforms in a stepped arrangement (platform travertines P0 to P9 in Fig. 5a) deposited on a slight slope toward the river valley and positioned between ca. 300 and 250 m below the glacis surface. Some of the travertine bodies seem to partially overlap, although others remain individualized (Fig. 5b). Most of these platforms lie

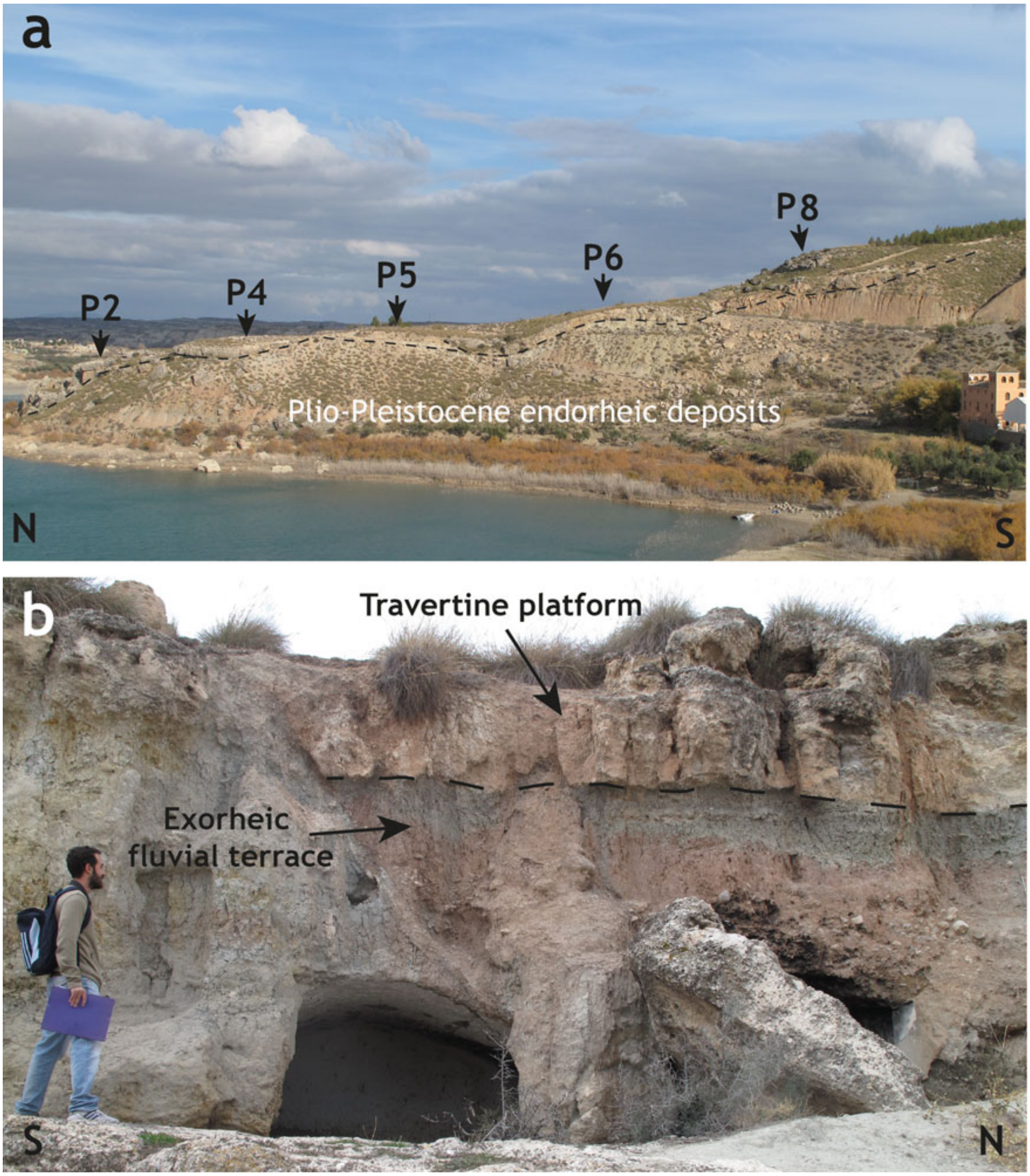

Figure 6. (**a**) Panoramic view showing the stepped arrangement of the Zújar travertine platforms formed in the Guadiana Menor River valley. (**b**) Detail of a travertine platform deposited over the exorheic detrital sediments of a previous fluvial terrace.

unconformably over Plio-Pleistocene endorheic sediments. However, some of them precipitated over previous exorheic deposits consisting of fluvial terraces of the GMR valley after its fluvial incision (Fig. 5a).

According to the derived $^{234}U/^{230}Th$ ages, the oldest travertine is platform P8 (sample ZT-3), which is located 250 ± 10 m below the glacis surface and 70 ± 1 m above the present thalweg of the GMR (Fig. 5). The P8 travertine was dated to 240.8 +29.27/−24.04 ka.

Platform P2 (sample ZT-2) is located 275 ± 10 m below the glacis surface and 45 ± 1 m above the present thalweg (Fig. 5). We obtained a radiometric date of 109.04 +6.77/−6.43 ka for P2.

The lowest travertine platform (P1, sample ZT-1) is located 300 ± 10 m below the glacis surface and 20 ± 1 m above the present thalweg (Fig. 5). Samples from this lower terrace yielded an age of 78.87 +4.53/−4.37 ka.

Numerical age of the PAT

The PAT (Figs. 7 and 8) is a fluvial terrace found 65 km upstream from the capture area and located in the eastern sector of the GBB (Fig. 3) on the NW side of the GMR valley. It forms part of a set of four fluvial terraces (T1 to T4, from older to younger) deposited at different heights with respect to the present thalweg of the GMR (Fig. 7). Unfortunately, T1 facies were not appropriate for OSL

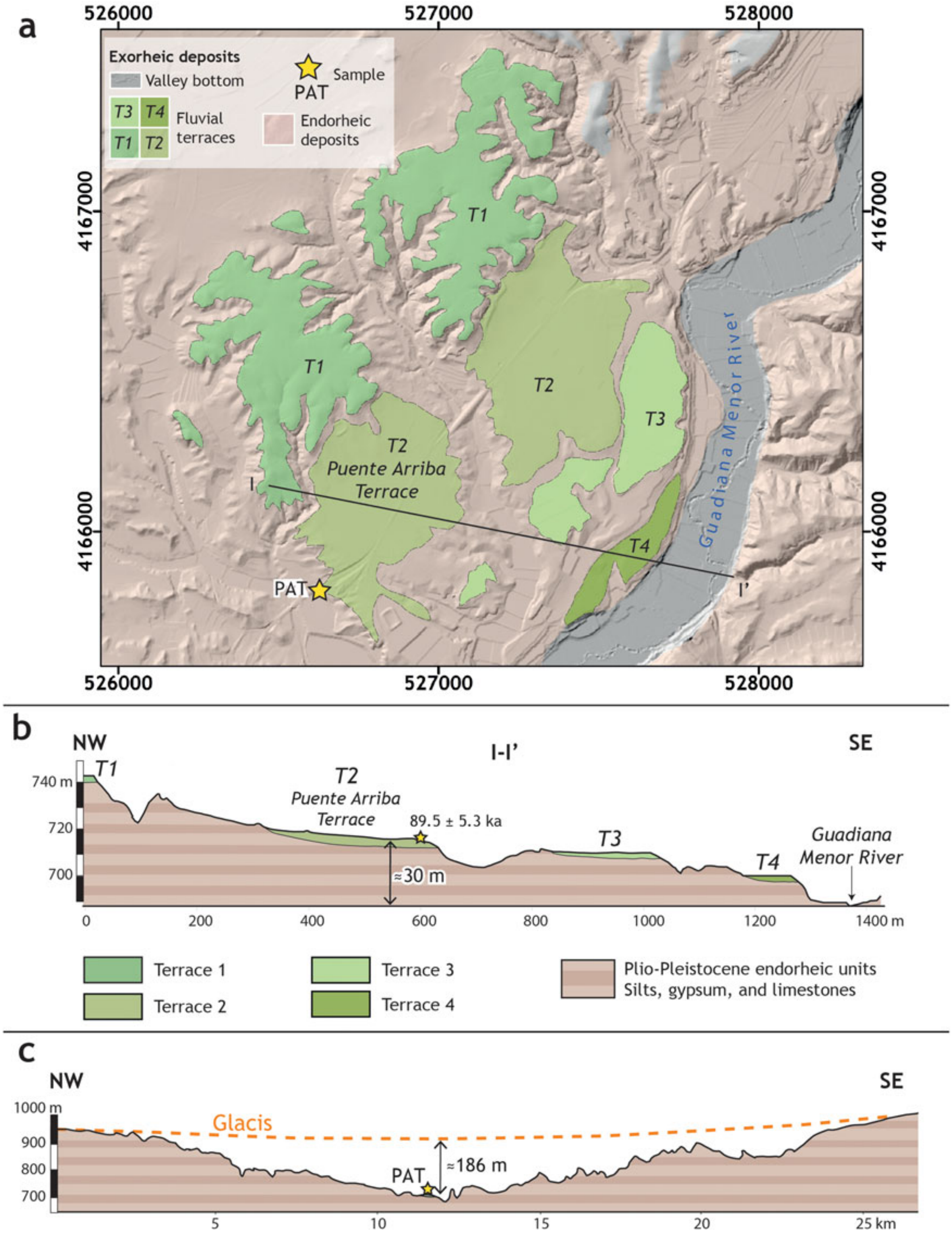

Figure 7. (**a**) Geologic map of the Puente Arriba fluvial terraces. (**b**) Geologic cross section along the Puente Arriba fluvial terraces (location in **a**). (**c**) Topographic profile showing the position of the dated terrace (T2) in relation to the glacis and the present thalweg.

dating. The dated PAT (T2) is located 186 ± 10 m below the glacis surface and 30 ± 1 m above the thalweg (Fig. 7). It is an unpaired fill fluvial terrace that reaches a thickness of up to 10 m. The terrace is partially eroded and composed of clast-supported conglomerate and gravel deposits. Locally, sandy levels can be observed. The exorheic deposit of the PAT unconformably overlies Lower Pleistocene endorheic deposits. OSL dating of the PAT provided an age of 89.5 ± 5.3 ka (Table 1).

When Was The GBB Captured? Insights From New Exorheic Ages

In this section, we discuss the meaning of our new numerical dates in terms of the age of the GBB capture. The time frame in which an internally drained basin is captured is constrained between the age of the youngest endorheic deposits and the oldest exorheic ones (Figs. 9–11). Therefore, to accurately date capture

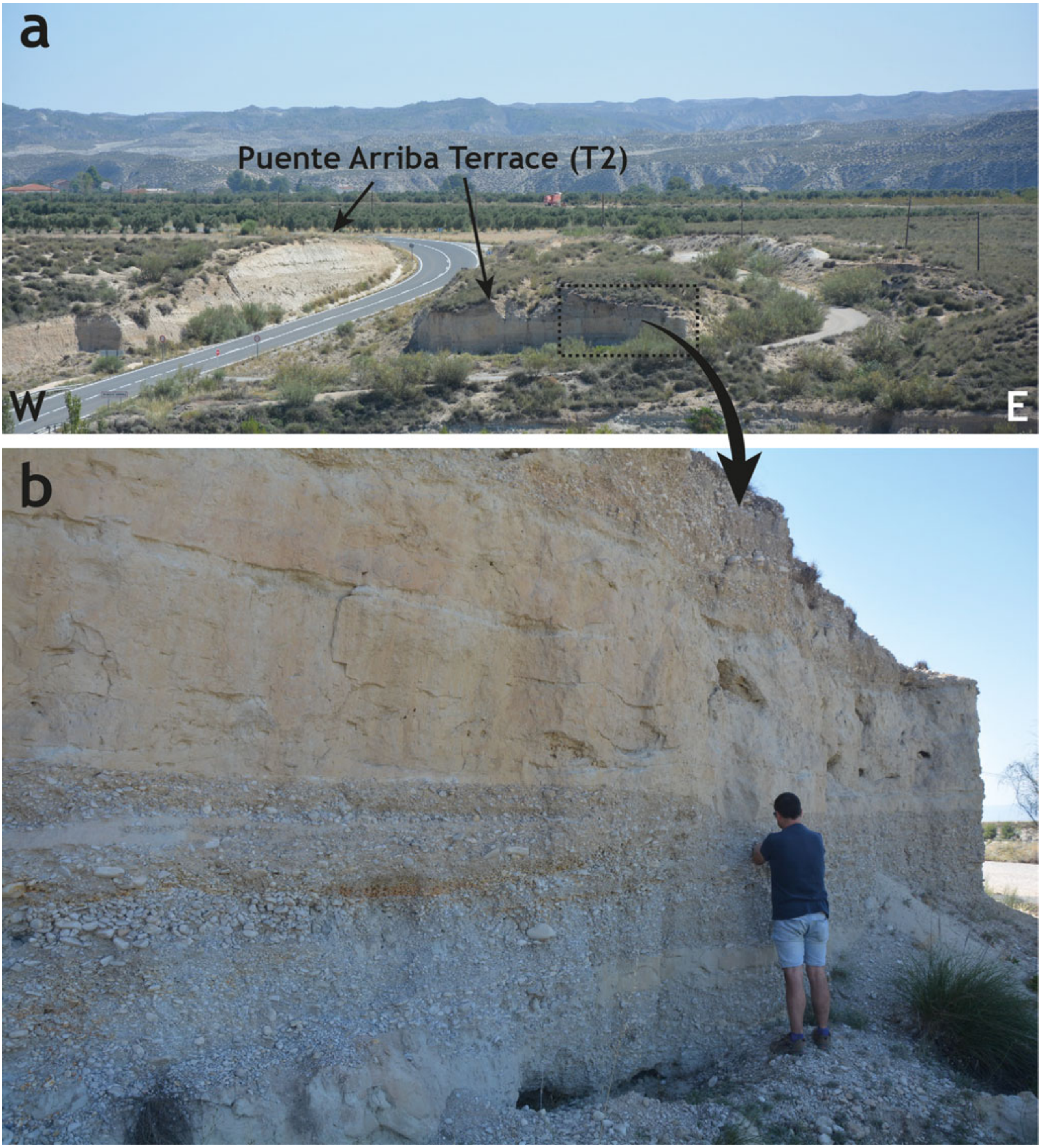

Figure 8. (**a**) Panoramic view of the Puente Arriba fluvial terrace. (**b**) Detail of the sampling site (upper level of fine sediments).

processes, effort must be put into dating these constraining horizons.

New numerical ages acquired in this work fell in a time range between 24.08 +29.26/−24.04 and 78.87 + 4,53/−4,37 ka (Table 1). We thus provided the oldest numerical age to date for an exorheic deposit within the GBB. As described earlier, platform P8 is an exorheic deposit cropping out within the valley of the GMR (Figs. 5 and 9). Therefore, this travertine body was formed when the valley was already dissected approximately 250 m below the glacis surface. This age agreed with the ages of other exorheic travertines of the GBB such as the Alicún travertines (Díaz-Hernández and Juliá, 2006). The uppermost Alicún travertine platform is located 190 ± 10 m below the glacis and was dated as ca. 220–190 ka (Fig. 9).

Hence, the age of the Zújar travertine platform P8 represents an upper constraint for the fluvial capture of the GBB. This implies that the capture should be older than 240.8 +29.26/−24.04 ka. However, to estimate the age of the fluvial capture,

Table 1. List of samples and numerical ages obtained for the Zújar travertine platforms and the Puente Arriba Terrace using U/Th and optically simulated luminescence (OSL) methods, respectively.

OSL

Sample	Depth (m)	Moisture (%)	Dose rate (Gy/ka)	Equivalent dose (Gy)	(ka before 2015)
TPA-1	2	5	1.62 ± 0.07	144.8 ± 5.6	89.5 ± 5.3

U/Th

Sample	^{238}U (ppm)	^{232}Th (ppm)	^{234}U/^{238}U	^{230}Th/^{232}Th	^{230}Th/^{234}U	Nominal date (years BP)
ZT-1	0.17	0.12	1.45 ± 0.04	3.474 ± 0.19	0.53 ± 0.02	78,867 +4524/−4363
ZT-2	0.17	0.08	1.84 ± 0.05	8.704 ± 0.631	0.67 ± 0.03	109,043 +6766/−6433
ZT-3	0.12	0.18	1.83 ± 0.07	3.795 ± 0.136	1 ± 0.04	240,798 +29,265/−24,042

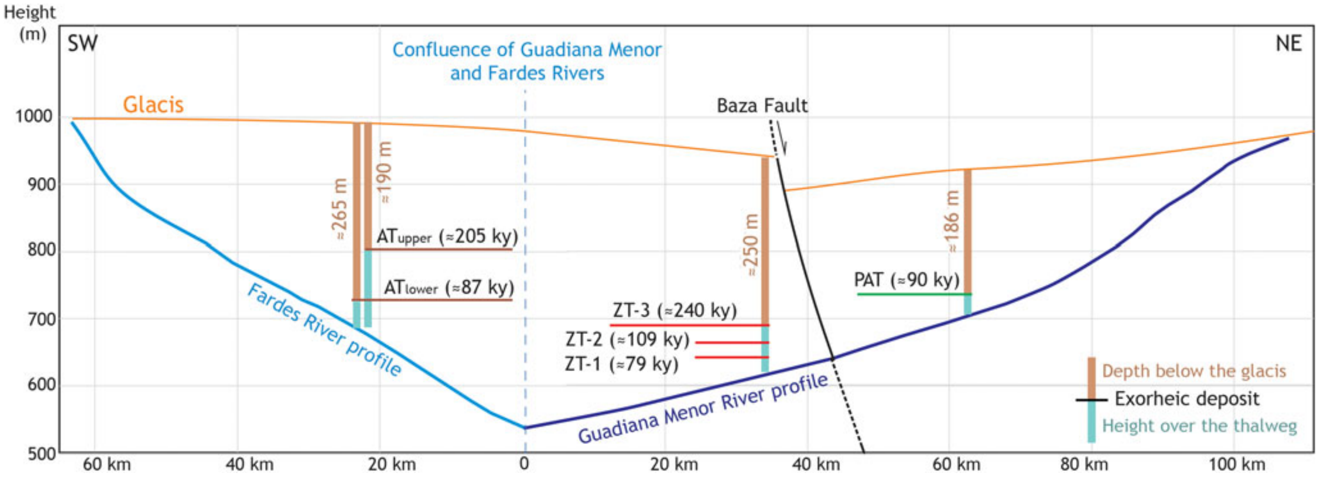

Figure 9. Numerical age and position of the exorheic deposits dated or included in the discussion of this study. They are depicted according to their depths below the glacis surface and the distances to the capture area, which is approximately the confluence between the Guadiana Menor and Fardes rivers (blue and purple longitudinal profiles). AT, Alicún travertines; ZT, Zújar travertines; PAT, Puente Arriba Terrace.

it is necessary to add to this age the time span required by the drainage network to dissect 250 m until the position of the travertine platform (Figs. 5, 9, and 11). Calculating this time span using incision rates may, however, be problematic, as they are highly sensitive to tectonics, climate changes, and local base-level variations. Extensive literature has proven that these forcings do

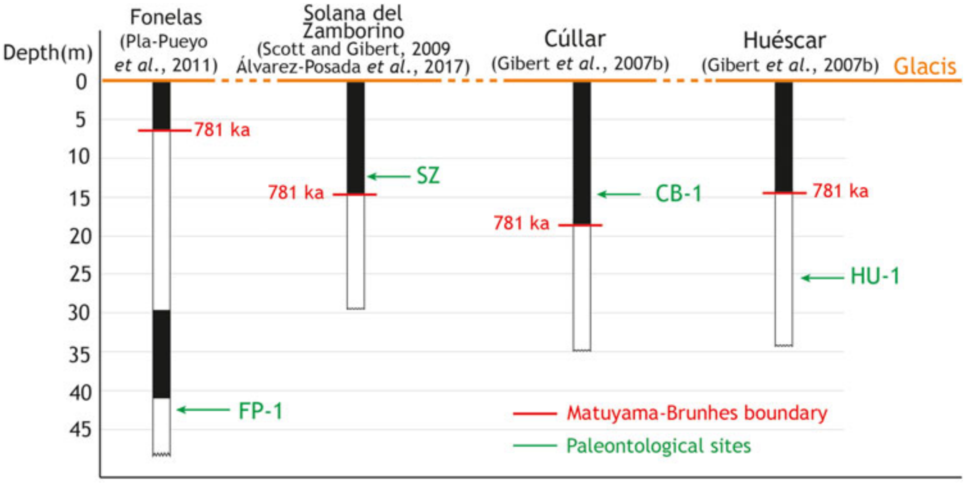

Figure 10. Sediment thickness between the glacis and the Matuyama-Brunhes reversal in different stratigraphic successions of the endorheic infilling of the Guadix-Baza Basin. The positions of the paleontological sites within these successions are indicated, along with the authors who identified the Matuyama-Brunhes reversal in each site (Gibert et al., 2007b; Scott and Gibert, 2009; Pla-Pueyo et al., 2011; Álvarez-Posada et al., 2017).

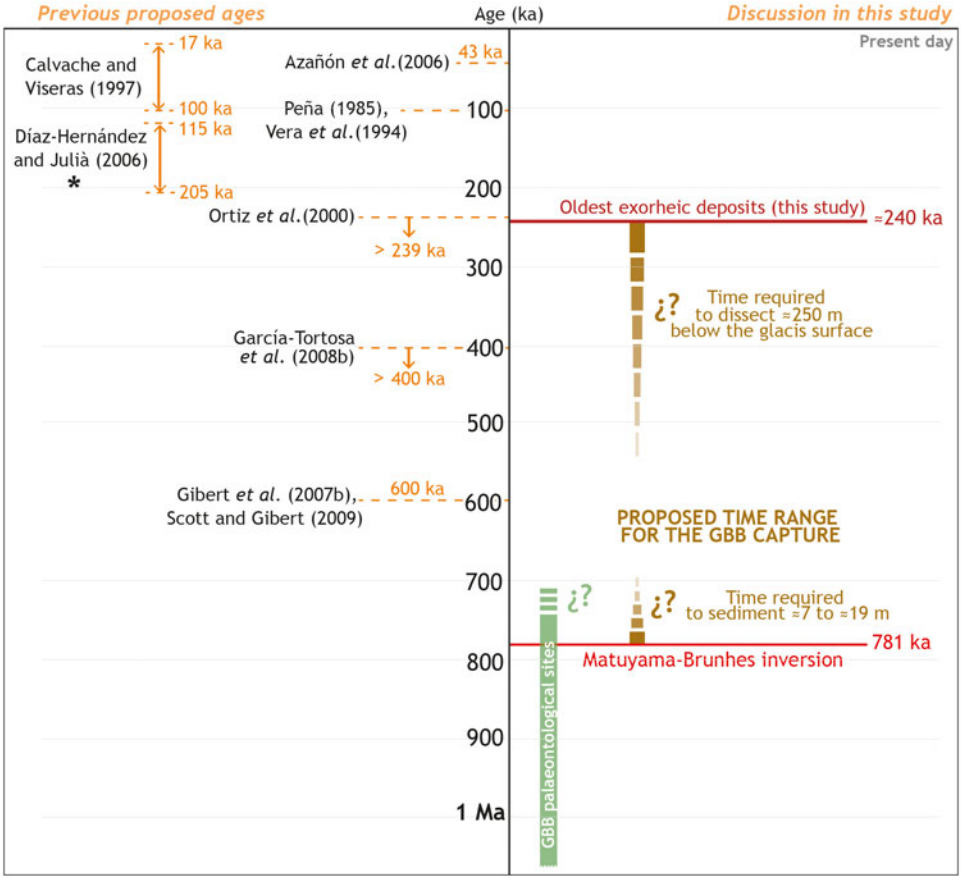

Figure 11. Chronological table of the Guadix-Baza Basin (GBB) capture event. The left side presents the different age proposals from previous works (Peña, 1985; Vera et al., 1994; Calvache and Viseras, 1997; Ortiz et al., 2000; Díaz-Hernández and Juliá, 2006; Azañón et al., 2006; Gibert et al., 2007b; García-Tortosa et al., 2008b; Scott and Gibert, 2009). The right side illustrates the time range we propose in this study for the capture process. The upper constraint of this range is the age of the oldest dated exorheic deposits presented in this work, with the additional time estimate for the drainage network to dissect the valley to the position of these deposits (ca. 250 m). The lower constraint is the Matuyama-Brunhes horizon plus the time required for the sedimentation of the thickness of endorheic deposits between the paleomagnetic reversal and the glacis. The ages of the youngest endorheic deposits are also supported by paleontological data (green bar).

not act linearly through time, which in turn implies a lack of linearity of incision rates along time and space, especially when dealing with time spans of more than hundreds of thousands of years (Pazzaglia et al., 1998; Whipple, 2001; Faust and Wolf, 2017). Table 2 shows incision rates estimated from the samples' position above the present thalweg, ranging between 0.2 and 0.6 mm/yr. If we use these incision rates to estimate the age of the capture assuming that they are constant, we obtain ages older than 780 ka. These ages of the capture assuming constant incision rates are not in agreement with the sedimentary record of the basin. Therefore, we think that the incision rates in the GBB are not linear but varied in time. Consequently, due to the high uncertainty derived from the use of incision rates, we considered that these rates were not suitable to estimate the age of the glacis and, therefore, of the basin capture. In any case, the Zújar travertines may have indicated an early capture event. This early capture was

Table 2. Incision rates estimated from the age of the samples and their position with respect to the current thalweg.

	A Height above thalweg (m)	B Age (ka BP)	C Incision rate (m/ka) from the sample position to the thalweg	D Sample location below the glacis (m)	E (D/C) Estimated Incision time (ka) from the glacis to the sample position[a]	F (E + B) Estimated capture age[b] (ka)
ZT-1	19–21	83–74	0.23–0.30	300	1304–1000	1387–1074
ZT-2	44–46	116–103	0.40–0.44	275	688–625	804–728
ZT-3	69–71	270–217	0.25–0.32	250	1000–781	1270–998
PAT	29–31	100–79	0.30–0.40	186	620–465	720–544
AT (upper)	114–116	220–190	0.51–0.61	190	373–311	593–501

[a] From the obtained incision rates, we estimate the time span required by the drainage network to dissect vertically to the position of the samples.
[b] This time span plus the age of the sample would give us an alleged age for the capture.

supported by the age of the PAT (89.5 ± 5.3 ka). This age implied that by this time, the GMR had already dissected 186 ± 10 m below the glacis surface at a distance of more than 60 km from the capture area (Fig. 9).

On the other hand, the age of the most recent endorheic deposits can provide a lower constraint on the age of the capture. Several controversial ages have been proposed for the younger horizons of the GBB. However, there is one datum consistently accepted for authors who worked in the GBB: the presence of the Matuyama-Brunhes reversal dated at ca. 781 ka. This paleomagnetic boundary is identified in several stratigraphic sections of the basin that also contain major paleontological sites. The Fonelas P-1 site (Arribas et al., 2001, 2009; Viseras et al., 2006; Pla-Pueyo et al., 2011) and the Solana del Zamborino site (Botella, 1975; Botella et al., 1976; Casas et al., 1976; Martín Penela, 1988; Scott and Gibert, 2009; Álvarez-Posada et al., 2017) are both in the western sector, while the CB1 and Huéscar 1 sites are both in the eastern sector of the basin (Ruiz-Bustos, 1976, 1984; Mazo et al., 1985; Alberdi and Bonadonna, 1989; Agustí et al., 1999; Gibert et al., 2007b; among others; Figs. 3 and 10). Figure 10 depicts the thickness of endorheic sediments over the Matuyama-Brunhes reversal and below the glacis surface. This thickness was ca. 7 m in Fonelas P-1, ca. 15 m in Solana del Zamborino, ca. 19 m in CB1, and ca. 15 m in Huéscar-1. Therefore, to estimate the age of the youngest endorheic deposits, we needed to add to the 781 ka of the paleomagnetic reversal time span necessary to deposit between 7 and 19 m of endorheic deposits (Fig. 10). Unfortunately, there is no consensus on sedimentation rates in the GBB. An example of this last statement arose in the Solana del Zamborino paleontological site. Scott and Gibert (2009) conducted a magnetostratigraphic analysis in this stratigraphic succession, identifying the Matuyama-Brunhes 15 m below the glacis. They used a sedimentation rate of 10 cm/ka to calculate the time span between the polarity reversal and the stratigraphic position of the site, obtaining an age of 770–750 ka for the Solana del Zamborino site. This sedimentation rate is obtained from a paleomagnetic and stratigraphic study in Cúllar (Fig. 3), in the easternmost part of the basin (Gibert et al., 2007b). Using a similar approach (paleomagnetism and sedimentation rates), Álvarez Posada et al. (2017) proposed an age of 480–300 ka for the Solana del Zamborino site based on a sedimentation rate of ca. 2 cm/ka. However, it has to be considered that this rate was obtained next to the Fonelas P1 site (Pla-Pueyo et al., 2011), where sedimentary facies (lacustrine facies) are different from those found in the Solana del Zamborino site (fluvial conglomerate facies). The use of sedimentation rates for calculating this time span is an unreliable approach, because it mainly depends on which number is selected and employed. This large disparity in the two proposed ages (Scott and Gibert, 2009; Álvarez Posada et al., 2017) prevents the use of this site to constrain the age of the GBB's capture.

Other data that may contribute to better constrain the age of the recent endorheic deposits of the GBB are the overall ages of the paleontological sites existing in the basin. According to the faunal assemblages collected within the endorheic sediments, only 3 out of more than 150 sites in the basin are either close to or younger than the Matuyama-Brunhes reversal: the Caniles, CB1, and Solana del Zamborino sites (Ruíz-Bustos, 1984; Guerra Merchán and Ruiz Bustos, 1992; Scott and Gibert, 2009; Álvarez-Posada et al., 2017). The other paleontological sites have ages much older than this paleomagnetic reversal. In addition, Demuro et al. (2015) reported ages of 570–420 ka for Huéscar 1 based on OSL analyses. However, other studies focusing on this site suggest an older age of 781 ka, supported by paleontological (Mazo et al., 1985; Alberdi and Bonadonna, 1989) and magnetostratigraphic data (Gibert et al., 2007b). Therefore, the Caniles, CB1, and Solana del Zamborino sites are considered the most recent sites in the basin (Maldonado-Garrido et al., 2017).

The Caniles site has an assigned age of ca. 781 ka based on its vertebrate faunal content (Guerra Merchán and Ruiz Bustos, 1992). The age of the CB1 site has been assigned as middle Pleistocene in different studies. Some authors propose an age between 500 and 750 ka based on its faunal assemblage (e.g., Ruiz Bustos, 1976; Alberdi and Bonadonna, 1989), while others propose an age of ca. 781 ka using paleomagnetism (Gibert et al., 2007b). However, considering the stratigraphic proximity of the site to the Matuyama-Brunhes reversal, it is more likely that its age is closer to that proposed by Gibert et al. (2007b).

In relation to calcrete ages of 350 ka (Díaz-Hernández and Juliá, 2006) and 42 ka (Azañón et al., 2006), it is necessary to consider that calcretes could have formed while the glacis was active or after it was abandoned. Consequently, we consider these ages are not reliable to estimate the age of the capture.

In conclusion, we consider that there are only two data sets robust enough to quantitatively constrain the age of the GBB's capture. The upper quantitative constraint is our age of 240.8 +29.27/−24.04 ka for the Zújar travertine platform P8 (the oldest dated exorheic deposit). The lower quantitative constraint is 781 ka, owing to the polarity reversal present in the upper part of the endorheic sedimentary succession.

The time span between ca. 240 and 781 ka could be refined by adding (1) the time necessary to dissect 250 m below the glacis until the position of the P8 travertine (Fig. 9) and (2) the time span necessary to sediment 7 to 19 m of endorheic deposits (sediment thickness between the Brunhes-Matuyama reversal and the glacis) (Fig. 10). As discussed earlier, we consider that incision rates are not suitable to quantitatively estimate the age of the basin capture. We also discussed that the controversy related to the sedimentation rates hinders a quantitative approach to calculate the age of the glacis. Further sedimentological and geomorphological analyses would be necessary to overcome these limitations. Therefore, we consider that a further refinement of the 781–240 ka time span using incision and sedimentation rates can only be addressed qualitatively.

Additional qualitative data for the lower constraint are the absence of paleontological sites younger than ca. 750 ka, except for the controversial age of the Solana de Zamborino site. Based on this, we postulate that the capture could have occurred close to the lower constraint, that is, close to 781 ka, well before the oldest proposed age of 600 ka by Gibert et al. (2007b).

An earlier capture would not contradict, however, the age of 600 ka proposed by Gibert et al. (2007b) for the glacis in the eastern sector. At the end of the endorheic stage, the headward erosion of a tributary of the Guadalquivir River reached the divide between the GBB and the Guadalquivir Basin. At that moment, erosion started in the GBB, leading to a new river, the Guadiana Menor. At this early stage, erosion in the GBB was initially constrained to a small area around the capture area. The first phase of the capture process was initiated when the abovementioned tributary of the Guadalquivir River reached a first river of the GBB fluvial network. As the headward erosion of the GMR proceeded, it eventually reached the main river of the western sector of the GBB, that is, the Fardes paleo-River. This moment was a milestone in the evolution of the basin, as it implied the capture of most of the drainage network of the western sector.

We hypothesize that the capture of the GBB was not a simple event because of the basin configuration related to the presence of the Baza Fault. Most likely, endorheic conditions persisted for a longer period in the eastern sector of the basin, located in the downthrown block of the Baza Fault. This fault could have kept the eastern sector of the GBB uncaptured, allowing continuous sedimentation, while the western sector of the basin was already captured. Subsequently, the eastward-migrating erosion along the western sector reached the Baza paleo-Lake. Consequently, the rivers previously draining toward the lake were incorporated into the new fluvial network, which drained to the west through the GMR. At this moment, the entire GBB became exorheic. An approximation to the evolution of the capture process in the basin could be deduced by comparing the available ages of exorheic deposits with their distance to the capture area and their position below the glacis surface (Fig. 9). However, we consider that relying solely on three dated exorheic deposits is insufficient for conducting this type of discussion. A further analysis, focused on dating a greater number of exorheic deposits throughout the entire GBB, would be necessary in the future to establish a much more precise evolutionary model along time and space.

Conclusions

In this study, we provide new numerical data to constrain the age of Guadix-Baza Basin capture. We dated a series of exorheic deposits that crop out within the valley of the Guadiana Menor River: three platforms of the Zújar travertines (P1, P2, and P8) and the Puente Arriba fluvial terrace.

The oldest Zújar travertine platform is dated to 240.8 +29.27/−24.04 ka. It corresponds to a platform at a position of 250 ± 10 m below the glacis and 70 ± 2 m above the present thalweg. On the other hand, the OSL dating of the Puente Arriba terrace provided an age of 89.5 ± 5.3 ka.

We thus provide the oldest age recorded to date for an exorheic deposit in the basin (ca. 240 ka), establishing a new upper constraint for Guadix-Baza Basin capture. We infer that basin capture took place before ca. 240 ka plus the additional time necessary for the Guadiana Menor River to incise 250 m down to the position of the Zújar travertine platform. Furthermore, our new dating, together with previous data, support the possibility that the capture occurred earlier than previously suggested. First, the presence of the Matuyama-Brunhes reversal, dated ca. 781 ka, close to the top of the endorheic succession of the basin represents a robust quantitative lower constraint. Additionally, the ages of the paleontological sites throughout the basin consistently fall within the range of approximately 750 ka or older (except for some ages proposed for the Solana del Zamborino site). Therefore, although we do not provide a precise age of the capture, several findings suggest that the capture event likely predates even the oldest proposed ages of 600 ka.

Funding. This research was funded by the Spanish Ministry of Science, Innovation and University (Research Projects RTI2018-100737-B-I00 and PID2021-127967NB-I00), Junta de Andalucía regional government (RNM325 research group), Generalitat Valenciana Research Project AICO/2021/196, and the University of Alicante (Research Project VIGROB053).

Competing Interests. The authors declare no competing interests.

References

Adamiec, G., Aitken, M.J., 1998. Dose-rate conversion factors: update. *Ancient TL* **16**, 37–50.

Agustí, J., 1986. Synthèse biostratigraphique du Plio-Pléistocène de Guadix-Baza Province de Granada, sudest de l'Espagne). *Geobios* **19**, 505–510.

Agustí, J., Lozano-Fernández, I., Oms, O., Piñero, P., Furió, M., Blain, H.A., López-García, J.M., Martínez-Navarro, B., 2015. Early to Middle Pleistocene rodent biostratigraphy of the Guadix-Baza Basin (SE Spain). *Quaternary International* **389**, 139–147.

Agustí, J., Oms, O., Parés, J.M., 1999. Calibration of the Early–Middle Pleistocene transition in the continental beds of the Guadix-Baza Basin (SE Spain). *Quaternary Sciences Reviews* **18**, 1409–1417.

Alberdi, M., Bonadonna, F.P., 1989. *Geología y Paleontología de la cuenca de Guadix-Baza*. Trabajos sobre el Neógeno-Cuaternario, CSIC 11. Museo nacional de ciencias naturales, Madrid.

Alfaro, P., Delgado, J., Sanz de Galdeano, C., Galindo Zaldívar, J., García-Tortosa, F.J., López Garrido, A.C., López Casado, C., Marín, C., Gil, A.J., Borque, M.J., 2008. The Baza Fault: a major active extensional fault in the central Betic Cordillera (South Spain). *International Journal of Earth Sciences* **97**, 1353–1365.

Alfaro, P., Sánchez-Alzola, A., Martin-Rojas, I., García-Tortosa, F.J., Galindo-Zaldívar, J., Avilés, M., López Garrido, A.C., *et al.*, 2021. Geodetic fault slip rates on active faults in the Baza sub-Basin (SE Spain): insights for seismic hazard assessment. *Journal of Geodynamics* **144**, 101815.

Álvarez Posada, C., Parés, J.M., Sala, R., Viseras, C., Pla-Pueyo, S., 2017. New magnetostratigraphic evident for the age Acheulan tools at the archaeo-paleontological site "Solana del Zamborino" (Guadix-Baza basin, S Spain). *Scientific Reports* **7**, 13495.

Arboleya, M.L., Babaut J., Owen, L.A., Teixell, A., Finkel, R.C., 2008. Timing and nature of Quaternary fluvial incision in the Ouarzazate foreland basin, Morocco. *Journal of the Geological Society of London* **165**, 1059–1073.

Arribas, A., Garrido, G., Viseras, C., Soria, J.M., Pla-Pueyo, S., Solano, J.G., Garcés M., Beamud, E., Carrión, J., 2009. A mammalian lost world in Southwest Europe during the late Pliocene. *PLoS ONE* **4**(9), 1–10.

Arribas, A., Riquelme, J.A., Palmqvist, P., Garrido, G., Hernández, R., Laplana, C., Soria, J.M., *et al.*, 2001. Un nuevo yacimiento de grandes mamíferos villafranquienses en la Cuenca de Guadix (Granada): Fonelas P-1, primer registro de una fauna próxima al límite Plio-Pleistoceno en la Península Ibérica. *Boletín Geológico y Minero* **112**, 3–34.

Azañón, J.M., Tuccimei, P., Azor, A., Sánchez-Almazo, I.M., Alonso-Zarza, A.M., Soligo, M., Pérez-Peña, J.V., 2006. Calcrete features and age estimates from U/Th dating: implications for the analysis of Quaternary erosion rates in the northern limb of the Sierra Nevada range (Betic Cordillera, Southeast Spain). In: Alonso-Zarza, A.M. y, Tanner, L.H. (Eds.), *Paleoenvironmental Record and Applications of Calcretes and Palustrine Carbonates. Geological Society of America Special Paper* **416**, 223–239.

Bischoff, J.L., Juliá, R., Mora, R., 1988. Uranium-series dating of the Mousterian occupation at Abric Romaní, Spain. *Nature* **332**, 68–70.

Botella, M., Vera, J.A., Porta, J., 1976. El yacimiento Achelense de la Solana de Zamborino. Fonelas. Granada (Primera campaña de excavaciones). *Cuadernos de Prehistoria de la Universidad de Granada* **1**, 1–45.

Botella, M.C., 1975. El cazadero achelense de la Solana de Zamborino (Granada). In: *Crónica del XIII Congreso Arqueológico Nacional, Huelva, 8-12 oct. 1973*. Seminario de Arqueología, Zaragoza, pp. 175–184.

Bridgland, D.R., Westaway, R., Hu, Z., 2020. Basin inversion: a worldwide Late Cenozoic phenomenon. *Global and Planetary Change* **193**, 103260.

Calvache, M.L., Viseras, C., 1997. Long-term control mechanisms of stream piracy processes in southeastern Spain. *Earth Surface Processes and Landforms* **22**, 93–105.

Casas, J., Ruano, J.A.P., Torres, J.A.V., 1976. Interpretación Geológica Y Estratigráfica Del Yacimiento De La "Solana Del Zamborino." *Cuadernos de Prehistoria y Arqueología de la Universidad de Granada* **1**, 5–15.

Castro, J., Martin-Rojas, I., Medina-Cascales, I., García-Tortosa, F.J., Alfaro, P., Insua-Arévalo, J.M., 2018. Active faulting in the central betic Cordillera (Spain): palaeoseismological constraint of the surface-rupturing history of the Baza Fault (central betic Cordillera, Iberian Peninsula). *Tectonophysics* **736**, 15–30.

Cruz-Sanjulián, J., García-Rossell, L., 1972. Características hidrogeológicas del sector del Jabalcón (Granada). *Boletín Geológico Minero* **83**, 68–80.

DeMets, C., Gordon, R.G., Argus, D.F., Stein, S., 1994. Effect of recent revisions to the geomagnetic reversal time scale on estimates of current plate motions. *Geophysical Research Letters* **21**, 2191–2194.

Demuro, M., Arnold, L.J., Parés, J.M., Sala, R., 2015. Extended-range luminescence chronologies suggest potentially complex bone accumulation histories at the Early-to-Middle Pleistocene palaeontological site of Huéscar-1 (Guadix-Baza basin, Spain). *Quaternary International* **389**, 191–212.

Díaz-Hernández, J.L., Juliá, R., 2006. Geochronological position of badlands and geomorphological patterns in the Guadix–Baza basin (SE Spain). *Quaternary Research* **65**, 467–477.

Faust, D., Wolf, D., 2017. Interpreting drivers of change in fluvial archives of the Western Mediterranean—a critical view. *Earth-Science Reviews* **174**, 53–83.

Fernández-Ibáñez, F., Pérez-Peña, J.V., Azor, A., Soto, J.I., Azañón, J.M., 2010. Normal faulting driven by denudational isostatic rebound. *Geology* **38**, 643–646.

Galindo-Zaldívar, J., Gil, A.J., Sanz de Galdeano, C., Lacy, M.C., García-Armenteros, J.A., Ruano, P., Ruiz, A.M., Martínez-Martos, M., Alfaro P., 2015. Active shallow extension in central and eastern Betic Cordillera from CGPS data. *Tectonophysics* **663**, 290–301.

García-Castellanos, D., Cruz Larrasoaña, J., 2015. Quantifying the post-tectonic topo-graphic evolution of closed basins: the Ebro basin (northeast Iberia). *Geology* **43**, 663–666.

García-Castellanos, D., Vergés J., Gaspar-Escribano, J., Cloetingh, S., 2003. Interplay between tectonics, climate, and fluvial transport during the Cenozoic evolution of the Ebro Basin (NE Iberia). *Journal of Geophysical Research* **108**(B7), 2347.

García Tortosa, F.J., Alfaro, P., Galindo Zaldívar, J., Gibert, L., López Garrido, A.C., Sanz de Galdeano, C., Ureña M., 2008b. Geomorphologic evidence of the active Baza Fault (Betic Cordillera, south Spain). *Geomorphology* **97**, 374–391.

García Tortosa, F.J., Alfaro, P., Galindo Zaldívar, J., Sanz de Galdeano, C., 2011. Glacis geometry as a geomorphic marker of recent tectonics: the Guadix-Baza Basin (South Spain). *Geomorphology* **125**, 517–529.

García Tortosa, F.J., Sanz de Galdeano, C., Alfaro, P., Jiménez-Espinosa, R., Jiménez-Millán, J., Lorite Herrera, M., 2008a. Nueva evidencia sobre la edad del tránsito endorreico-exorreico de la cuenca de Guadix-Baza. *Geogaceta* **44**, 211–214.

Gibert, L., Ortí, F., Rosell, L., 2007a. Plio-Pleistocene lacustrine evaporites of the Baza Basin (Betic Chain, SE Spain). *Sedimentary Geology* **200**, 89–116.

Gibert, L., Scott G., Martin, R., Gibert, J., 2007b. The Early to Middle Pleistocene boundary in the Baza Basin (Spain). *Quaternary Science Reviews* **26**, 2067–2089.

Guerra Merchán, A., Ruiz Bustos, A., 1992. Nuevos datos bioestratigráficos de los materiales continentales del sector suroriental de la Cuenca de Guadix-Baza. El yacimiento de Caniles. *Geogaceta* **11**, 76–78.

Hallstadius, L., 1984. A method for the electrodeposition of actinides. *Nuclear Instruments and Methods in Physics Research A* **223**, 266–267.

Heidarzadeh, G., Ballato, P., Hassanzadeh, J., Ghassemi, M.R., Strecker, M.R., 2017. Lake overspill and onset of fluvial incision in the Iranian Plateau: insights from the Mianeh Basin. *Earth and Planetary Science Letters* **469**, 135–147.

Jiménez de Cisneros, C., 1994. Geoquímica de carbonatos relacionada con etapas de emersión. PhD thesis. University of Granada, Granada.

Maldonado-Garrido, E., Piñero, P., Agustí, J., 2017. A catalogue of the vertebrate fossil record from the Guadix-Baza Basin (SE Spain). Spanish *Journal of Palaeontology* **32**, 207–236.

Martín Penela, A., 1988. Los grandes mamíferos del yacimiento Achelense de la Solana del Zamborino, Fonelas (Granada, España). *Antropología y Paleoecología Humana* **5**, 29–187.

Martín Rojas, I., Alfaro, P., Galindo-Zaldívar, J., Borque, M.J., García-Tortosa, F.J., Sanz de Galdeano, C., Avilés, M., *et al.*, 2023. Insights of active extension within a collisional orogen from GNSS (Central Betic Cordillera, S Spain). *Tectonics* **42**, e2022TC007723.

Mather, A.E., 2000. Adjustment of a drainage network to capture induced base- level change: an example from the Sorbas Basin, SE Spain. *Geomorphology* **34**, 271–289.

Mazo, A.V., Sesé, C., Ruiz-Bustos, A., Peña, J.A., 1985. Geología y paleontología de los yacimientos plio-pleistocenos de Huéscar (Depresión de Guadix-Baza). *Estudios Geológicos* **41**, 467–493.

Medina-Cascales, I., Martin-Rojas, I., García-Tortosa, F.J., Peláez, J.A., Alfaro, P., 2020. Geometry and kinematics of the Baza Fault (central Betic Cordillera, South Spain): insights into its seismic potential. *Geologica Acta* **18**(11), 1–25.

Merritts, D.J., Vincent, K.R., Wohl, E.E., 1994. Long river profiles, tectonism, and eustasy; a guide to interpreting fluvial terraces. *Journal of Geophysical Research* **99**(B7), 14031–14050.

Moral, F., Balanyá, J.C., 2020. Recent fault-controlled glacis deformation and its role in the fluvial capture of the Guadix-Baza basin (Betic Cordillera, southern Spain). *Geomorphology* **363**, 107226.

Murray, A.S., Wintle, A.G., 2000. Luminescence dating of quartz using an improved single-aliquot regenerative-dose protocol. *Radiation Measurement* **32**, 57–73.

Nocquet, J., 2012. Present-day kinematics of the Mediterranean: a comprehensive overview of GPS results. *Tectonophysics* **579**, 220–242.

Ortiz, J.E., Torres, T., Llamas, J.F., Canoira, L., García-Alonso, P., García de la Morena, M.A., Lucini, M., 2000. Dataciones de algunos yacimientos paleontológicos de la cuenca de Guadix-Baza (sector de Cúllar-Baza, Granada, España. y primera estimación de edad de la apertura de la cuenca mediante el método de racemización de aminoácidos. *Geogaceta* **28**, 109–112.

Pazzaglia, F.J., Gardner, T.W., Merritts, D.J., 1998. Bedrock fluvial incision and longitudinal profile development over geologic time scales determined by fluvial terraces. *Geophysical Monograph Series* **107**, 207–235.

Peña, J.A., 1985. La depresión de Guadix-Baza. *Estudios Geológicos* **41**, 33–46.

Pérez-Peña, J.A., Azañón, J.M., Azor, A., Tuccimei, P., Della Seta, M., Soligo, M., 2009. Quaternary landscape evolution and erosion rates for an intramontane Neogene basin (Guadix–Baza basin, SE Spain). *Geomorphology* **106**, 206–218.

Pla, S., Viseras, C., Soria, J.M., Tent-Manclús, J.E., Arribas, A., 2011. A stratigraphic framework for the Pliocene-Pleistocene continental sediments of the Guadix Basin (Betic Cordillera, S. Spain). *Quaternary International* **243**, 16–32.

Prescott, J.R., Hutton, J.T., 1994. Cosmic ray contributions to dose rates for luminescence and ESR dating: large depths and long term time variations. *Radiation Measurements* **23**, 497–500.

Rosenbauer, R.J., 1991. UDATE1: a computer program for the calculation of uranium-series isotopic ages. *Computer and Geosciences* **17**, 45–75.

Ruiz Bustos, J.A., 1976. Estudio Sistemático y Ecológico sobre las faunas del Pleistoceno Medio en las depresiones Granadinas. El yacimiento de Cúllar de Baza-1. Trabajos y Monografías, Dpto. *Zoología, University of Granada* **1**, 1–300.

Ruiz-Bustos, J.A., 1984. El yacimiento paleontológico Cúllar Baza-1. *Investigación y Ciencia* **91**, 20–28.

Sanz de Galdeano, C., 1983. Los accidentes y fracturas principales de las cordilleras Béticas. *Estudios Geológicos* **39**, 157–165.

Sanz de Galdeano, C., García-Tortosa, F.J., Peláez J.A., Alfaro, P., Azañón, J.M., Galindo-Zaldívar, J., López Casado, C., López Garrido, A.C., Rodríguez-Fernández, J., Ruano, P., 2012. Main active faults in the Granada and Guadix-Baza Basins (Betic Cordillera). *Journal of Iberian Geology* **38**, 209–223.

Scott, G., Gibert, L., 2009. The oldest hand-axes in Europe. *Nature* **461**, 82–85.

Serpelloni, E., Vannucci, G., Pondrelli, S., Argnani, A., Casula, G., Anzidei, M., Baldi, P., Gasperini, P., 2007. Kinematics of the Western Africa-Eurasia plate boundary from focal mechanisms and GPS data. *Geophysical Journal International* **169**, 1180–1200.

Silva, P.G., Roquero, E., López-Recio, M., Huerta, P., Martínez-Graña, A.M., 2017. Chronology of fluvial terrace sequences for large Atlantic rivers in the Iberian Peninsula (Upper Tagus and Duero drainage basins, Central Spain). *Quaternary Science Reviews* **166**, 188–203.

Sobel, E.R., Hilley, G.E., Strecker, M.R., 2003. Formation of internally drained contractional basins by aridity-limited bedrock incision. *Journal of Geophysical Research: Solid Earth* **108**(B7). http://dx.doi.org/10.1029/2002jb001883.

Soria, J.M., Fernádez, J., Viseras, C., 1999. Late Miocene stratigraphy and palaeogeographic evolution of the intramontane Guadix Basin (Central Betic Cordillera, Spain): implications for an Atlantic-Mediterranean connection. *Palaeogeography, Palaeoclimatology, Palaeoecology* **151**, 255–266

Stokes, M., Mather, A., Rodes, A., Kearsey, S., Lewin, S., 2018. Anatomy, age and origin of an intramontane top basin surface (Sorbas Basin, Betic Cordillera, SE Spain). *Quaternary* **1**, 15.

Struth, L., Garcia-Castellanos, D., Viaplana-Muzas, M., Vergés, J., 2019. Drainage network dynamics and knickpoint evolution in the Ebro and Duero basins: from endorheism to exorheism. *Geomorphology* **327**, 554–571.

Talvitie, N.A., 1972. Electrodeposition of actinides for alpha spectrometric determination. *Analytical Chemistry* **44**, 280–283.

Toro-Moyano, I., Barska, D., Cauche, D., Celiberti V., Grégoire, S., Lebegue, F., Moncel, M.H., Lumley, H. de, 2011. The archaic stone tool industry from Barranco León and Fuente Nueva 3 (Orce, Spain): evidence of the earliest hominin presence in southern Europe. *Quaternary International* **243**, 80–91.

Toro-Moyano, I., Martínez-Navarro, B., Agustí, J., Souday, C., Bermúdez de Castro, J.M., Martinón-Torres, M., Fajardo, B., *et al.*, 2013. The oldest human fossil in Europe, from Orce (Spain). *Journal of Human Evolution* **65**, 1–9.

Vera, J.A., 1970. Estudio estratigráfico de la depresión de Guadix-Baza. *Boletín Geológico y Minero* **81**, 429–462.

Vera, J.A., Rodríguez, J., Guerra A., Viseras C., 1994. La cuenca de Guadix-Baza. *Documents et Travaux de l'IGAL* **14**, 1–17.

Viseras, C., 1991. Estratigrafía y Sedimentología del relleno aluvial de la Cuenca de Guadix (Cordilleras Béticas). PhD thesis. University of Granada, Granada.

Viseras, C., Soria, J.M., Durán, J.J., Pla, S., Garrido, G., García-García, F., Arribas, A., 2006. A large-mammal site in a meandering fluvial context (Fonelas P-1, Late Pliocene, Guadix Basin, Spain). Sedimentological keys for its paleoenvironmental reconstruction. *Palaeogeography, Palaeoclimatology, Palaeoecology* **242**, 139e168.

Whipple, K.X., 2001. Fluvial landscape response time: how plausible is steady-state denudation? *American Journal of Science* **301**, 313–325.